www.nature.com/scientificdata

scientific data

Check for updates

OPEN

DATA DESCRIPTOR

# A Submarine Landslides Database of Calabrian Continental Margins (Central Mediterranean Sea)

Marco Bianchini[1,2] ✉, Francesco Latino Chiocci[2,3] & Silvia Ceramicola[1]

**Submarine landslides are complex and widespread natural events occurring all over the world, in every latitude and depth. Understanding the genesis and evolution of submarine landslides requires interpreting the nature of the seafloor, on which these landslides occur. This work presents a large database on the submarine landslides distribution along the Ionian and Tyrrhenian continental margins of Calabria (southern Italy), based high-resolution bathymetric data. An area of over 12,000 km$^2$ in the central Mediterranean Sea, characterized by active tectonics, was analyzed using specific standards. A total of 1,945 submarine landslides has been mapped, and several morphometric parameters describing the size, shape and geometry have been measured and analyzed. Such datasets may allow us to investigate the relationship between landslides morphology, spatial distribution, and the possible controlling factors of submarine landslides.**

## Background & Summary

Submarine landslides are widespread natural events that occur along both active and passive continental margins, ranging from shallow to deep waters, and even on gentle inclined slopes of a just few degrees[1]. Although ubiquitous, these phenomena are preferentially located on specific seafloor morphologies, such as submarine canyons[2,3], river deltas[4,5], fjords[6], volcanic islands, open slope[7] and tectonically-controlled oceanic scarps[8,9].

Seafloor morphology, lithology, mechanical properties of sediment, and the type of triggering event can influence the geometrical and dimensional variability of the submarine landslides[10], which as a result show similar characteristics in a given area, depending on the geological environment[11,12].

Submarine landslides have significantly influenced the evolution of continental margins in the past and continue to shape them today[13], also representing major geological hazards for marine infrastructures and coastal settlements. Offshore infrastructure, such as telecommunications cables, oil and gas pipelines, wind farms and other renewable energy plants are particularly exposed[14]. In the study area, despite the widespread presence of submarine cables along Calabrian margins, only one documented case of cable failure is reported to date. This occurred in 1977, in association with a submarine landslide occurred in the Gioia Tauro canyon head that evolved into a turbidity current that broke the cable at approximately 600 m water depth, around 15 km from the source area[15]. Moreover, along coastal areas, increasing urbanization and infrastructures development[16] can amplify the risk of instability and in some cases, even trigger it due to human error or poorly planned engineering works, potentially leading to tsunami events, as occurred in Gioia Tauro in 1977[17] and in Nice in 1979[18].

Over the past two decades, several studies at local and regional scale have systematically mapped and characterized submarine landslides along continental margins[19]. Notable examples include investigations along the Atlantic margin of the United States[20,21], in the Mediterranean[22], along the Iberian margins[23–25], and on the Australian margin[26,27]. In Italy, the MaGIC project (Marine Geohazard along the Italian Coasts, https://www.protezionecivile.gov.it/en/approfondimento/progetto-magic-marine-geohazards-along-italian-coasts-0/) marked a milestone in seabed mapping efforts[28], with an extensive acquisition of high-resolution bathymetric data, coupled with the implementation of standardized procedures for the systematic mapping of marine geohazard features. However, the scope of the mapping was the identification of geohazard features without providing detailed morphological characterization or interpretation. This study, based on the MaGIC dataset,

[1]OGS - National Institute of Oceanography and Applied Geophysics, Borgo Grotta Gigante 42C, 34010, Trieste, Italy. [2]Department of Earth Sciences, Sapienza University, Piazzale Aldo Moro 5, 00185, Rome, Italy. [3]CCNR - Institute of Environmental Geology and Geo-Engineering, National Research Council, Rome, Italy. ✉e-mail: marco.bianchini@uniroma1.it

originally reanalyzed all the features related to marine landslides, representing the first attempt in Italy to develop a detailed and comprehensive database[29] of submarine landslides, using the Calabrian continental margins as a pilot area[30,31]. The bathymetric dataset has been fully reinterpreted to ensure a consistent and standardized depiction of landslide features and the morphometric parameters measurement. In fact, although submarine landslides (and other geohazard features) were mapped according to common cartographic standards in MaGIC project, it became evident from the early stages of this study that interpretations varied among analysts across different areas, resulting in a lack of consistency. Moreover, any observation (especially if not originally designed for use in a comparative morphometric database) inevitably involved a high degree of subjectivity. Given complex morphologies and coalescing scars typical of submarine landslides, careful and consistent interpretation by the same operator is essential to minimize the risk of overestimating landslide features among different areas.

The study area covers approximately 7,800 km² in the Ionian Sea and 4,500 km² in the Tyrrhenian Sea, between longitudes 15°25′00″E and 17°33′00″E, and latitudes 38°18′00″N and 40°07′00″N. A total of 1,945 submarine landslides has been mapped and morphometrically characterized: 1,301 on the Ionian continental margin and 644 on the Tyrrhenian continental margin (Fig. 1)

The continental margins of Calabria (southern Italy) are among the most geodynamically active sectors of the central Mediterranean[32]. This region lies at the complex convergent boundary between the African and Eurasian plates, where the subduction of the Ionian lithosphere beneath the southern Apennines and Calabria has driven intense tectonic activity over geological time[33,34]. The resulting geodynamic setting is characterized by a combination of compressional and extensional tectonics, crustal thinning, widespread active faulting, high frequency seismicity and significant vertical movements, including uplift and subsidence that have shaped both the subaerial and submarine landscape[35–37] (Fig. 1S). The Calabrian arc plays a central role in the geodynamics of the region, giving rise to a complex forearc system and an accretionary prism that extends offshore into the Ionian[38]. Since the Tortonian, this subduction has also led to the opening of the Tyrrhenian back-arc basin, while the Ionian margin lies within the forearc zone, overlying an actively deforming accretionary wedge[39]. The persistent tectonic activity has resulted in narrow or absent continental shelves, to rapid transition from the subaerial mountain range to steep submarine continental slopes, often exceeding 30°[40]. The shelf breaks are carved by numerous submarine canyons and channels, which, on both the Ionian and Tyrrhenian margins, often reach a few hundred or tens of meters from the coastline[40,41]. These canyons are actively evolving through retrogressive erosion and show oversteepened, unstable flanks, making them particularly prone to landslides[2,42]. However, the hazard extends beyond the canyons themselves; the surrounding seafloor, marked by steep slopes, active tectonics, sediment accumulation and vertical movements (uplift rates reaching up to 1 mm/year since the Middle Pleistocene[35,43,44]), is similarly prone to landsliding. In these contexts, the interplay between tectonic forcing, sediment dynamics, and morphological controls creates an environment with a high potential for geohazards, including submarine landslides capable of generating tsunamis. Understanding this complex tectonic framework is therefore crucial for assessing the evolution of the Calabrian margins and for evaluating the risks posed to coastal communities and marine infrastructures[30,31].

The database presented in this manuscript represents the first comprehensive characterization of submarine landslides ever conducted along the Italian continental margins and may represent the foundation for future expansions to other regions, with the aim of developing a nationwide submarine landslide geodatabase. As regards the area of study, the database can help to understand submarine landslides along the Calabrian margins, by analyzing a high number of submarine landslides in different physiographic settings and with a wide morphological variability. While previous studies have focused on the characterization of single events or specific areas, this inventory provides a comprehensive dataset that encompasses the spatial distribution of submarine landslides over very wide areas and integrates morphometric analysis. By providing to the scientific community new data on the spatial and morphological characteristics of submarine landslides, this research will contribute to improving landslides hazard assessments and management strategies.

## Methods

The workflow was organized in 3 steps as follows: (1) retrieving bathymetric data, (2) original mapping and interpretation of submarine landslide and (3) measurement of morphometric parameters.

**Bathymetric data.** The Digital Elevation Models (DEMs) used in this study originate from data acquired during oceanographic cruises in the framework of the MaGIC project between 2007 and 2013, as well as data previously collected by different Italian research institutes; OGS (National Institute of Oceanography and Applied Geophysics), CNR (National Research Council), and CoNISMa (National Inter-University Consortium for Marine Sciences).

For this study, DEM data in ASCII (.asc) and GeoTIFF (.tiff) formats were used, with horizontal resolution varying with depth. DEM resolution is the following: 5 m for data between 0 and 200 m depth (~750 km$^2$), 10 m resolution for data between 200 and 500 m depth (~2,000 km$^2$), and 20 m resolution for bathymetry deeper than 500 m (~10,000 km$^2$). The raster datasets were divided by resolution and location (7 for the Tyrrhenian zone and 16 for the Ionian zone).

The bathymetric data are accessible from the Italian Civil protection website ((https://www.protezionecivile.gov.it/en/approfondimento/progetto-magic-marine-geohazards-along-italian-coasts-0), but at resolution of 50 m, 100 m and 200 m as published in the MaGIC atlas[45]. The high-resolution data is available upon request to the authors. However, given the scope of this study, high-resolution bathymetric data of the mapped submarine landslides source and deposit areas with a buffer of 50 m are provided in the Zenodo repository (https://doi.org/10.5281/zenodo.17422269) to enable independent verification of the database.

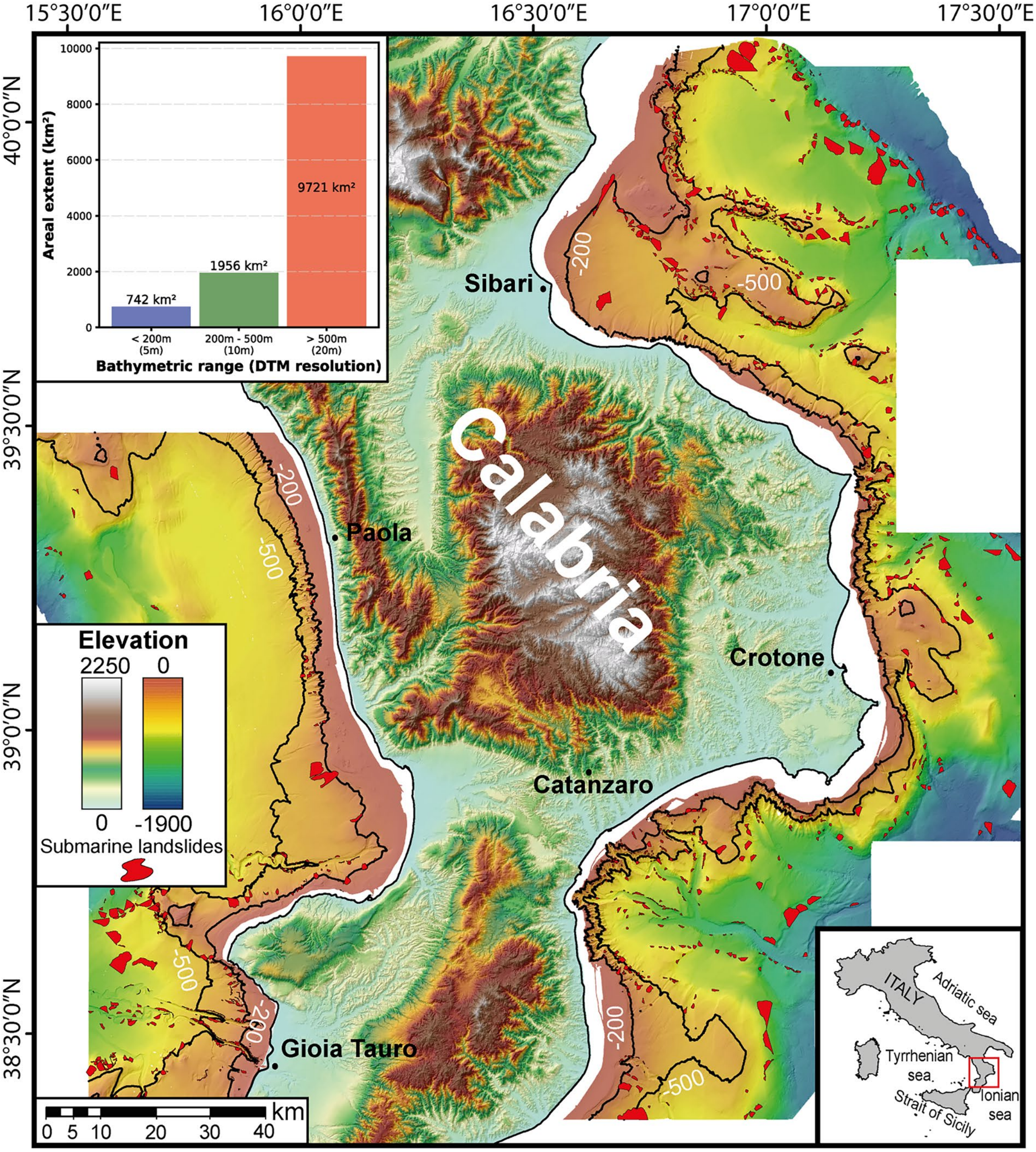


**Fig. 1** Map of the study area, red polygons represent the submarine landslides included in the database[29], 200 and 500 m depth contours are represented, they board different grid size of DEM, respectively of 5 m (<200), 10 m (200–500), 20 m (>500). The histogram on the upper left indicates the areal extension of each depth interval and the consequent grid resolution.

**Landslide mapping.** The mapping of the submarine landslides was carried out manually using 2D and 3D visualization in the Global Mapper software (https://www.bluemarblegeo.com/global-mapper/).

Three vector layers were defined and measured (Fig. 2) for each submarine landslide:

- **Scar/Crown (polyline)**: The upper boundary of the submarine landslide's failure niche, located between the undisturbed material and the mobilized material.
- **Source Area (derived polygon)**: The area that is encompassed by the landslide scar from which the failed mass was evacuated.
- **Deposit Area (polygon)**: The downslope area occupied by landslide material, with the lower boundary represented by the toe slope break. Depending on the environment (e.g. canyon slopes or steep slopes) where submarine landslides occur, the deposit area can be lost or, in other cases, undepictable using only bathymetric data.

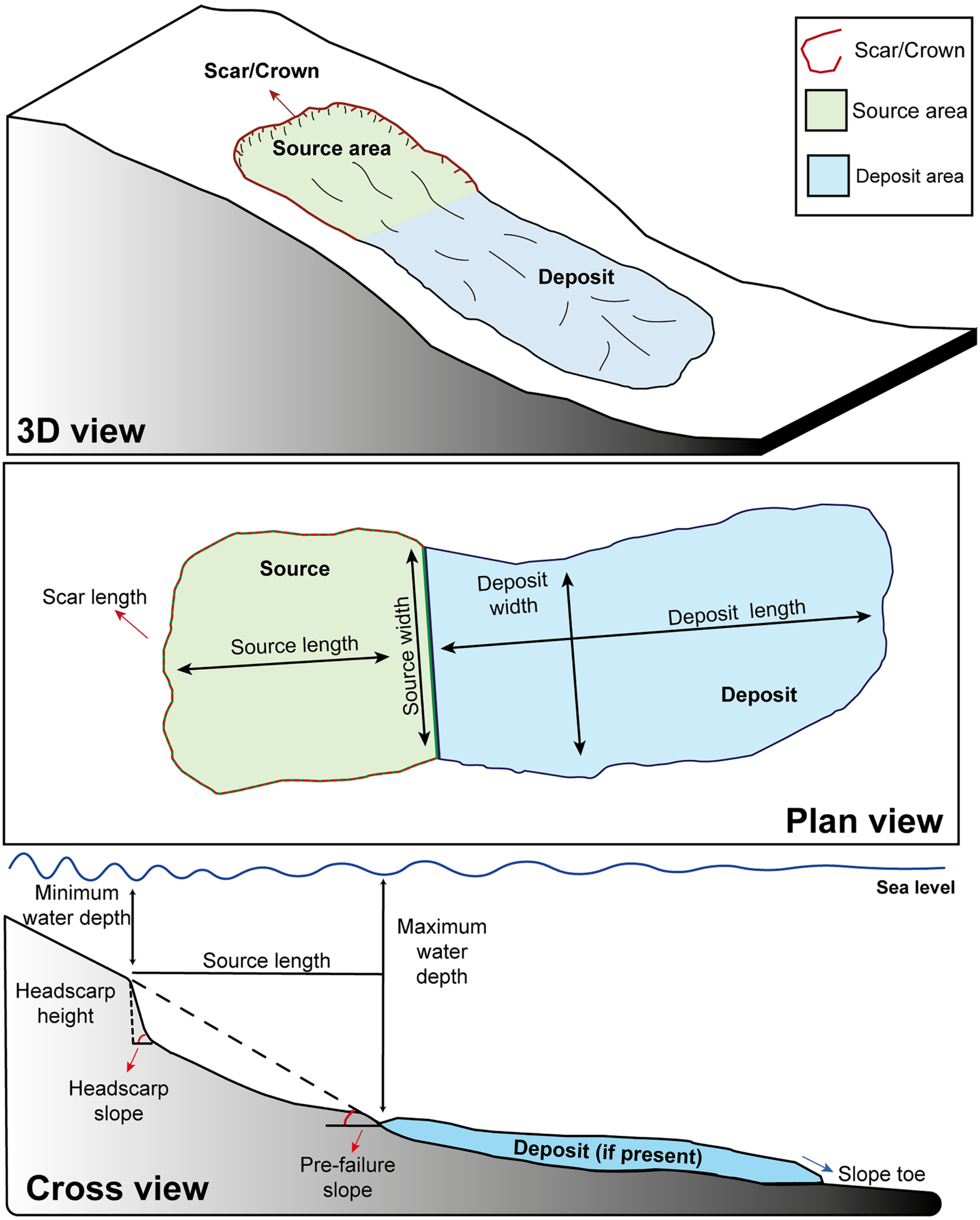


**Fig. 2** Sketches of the measured submarine landslide parameters. At the top, there is a 3D representation, in the center a plan view and below a cross-section along the run-out direction.

Given that deposits were catalogued for less than 1% of the total mapped landslides (18 features), source areas were standardized by delineating them from the scar/crown polyline. Consequently, mapped polygons for source and deposit areas may overlap when morphological evidence indicates that part of the mobilized sediment did not flow beyond the source area, remaining within the scar/crown extent.

**Morphometric parameters.** Once the mapping of a given submarine landslide was completed, the following step was the measurement of its morphometric attributes. The selection of attributes to be measured was made through an extensive literature review and based on previously works[22,46], leading to the selection of 40 attributes

(Fig. 2), 6 of those are operative (e.g., "ID," "Reference"…) and 34 are morphometric, divided between the 3 vector layers (Table 1). Further illustrations showing how some of the morphometric parameters were measured on example areas of the original bathymetric data are provided in the supplementary material (Fig. 2S).

The measurement of morphometric attributes was carried out either by using automatic tools allowed by the software and partly through standardized manual measurements (see Table 1 for descriptions), aiming to achieve the most possible homogenous landslide characterization. The volume values were calculated separately and then reintegrated into the complete dataset[29] (*see* the "Volume calculation" section for a detailed description of the process).

**Volume calculation.** The volume of a landslide was computed by comparing measured post-event morphology with reconstructed pre-event conditions. In fact, the bathymetric data provides information about the post-failure state only. Therefore, it was necessary to generate a bathymetric surface representing the pre-landslide conditions, using a method proposed by Gamboa *et al.*[25]. The generation of pre-failure surface required several steps and the use of various tools available in QGIS (https://qgis.org/) as follows. First, a copy of the DEM was created. Then the raster was clipped using a mask made up of the source area to obtain a DEM of the unfailed area. Three different methods were then used to create the hypothetical pre-failure surface. The first two methods utilized existing tools such as: 1) data gaps fill using a "multilevel b-spline" algorithm[47,48] (BS), with a 5 m × 5 m grid resampling, and 2) data gaps fill using a "close gaps" module[48] (CG). The third method, used when the automatic tools were unable to generate ideal surfaces (geometric aberration, over or underestimation of the pre-failure morphology), was a manual reconstruction of the pre-failure surface by linearizing the contour/isobaths inside the polygonal boundary of the "Source areas" and subsequently interpolating to generate a new DEM. The reconstructed surfaces were compared, and the one that best represented the overall geometry of the surrounding morphology was selected. The selected surface was filtered, and the low-frequency component (noise minimization) of the raster was selected as the model for pre-failure morphology. The volume of the source areas of the submarine landslides was then calculated using the "Volume Calculation Tool" plugin in QGIS, with the original bathymetry as the basal surface and the reconstructed surface as the upper surface (Fig. 3).

## Data Records

The dataset is available at "Submarine Landslides Database along the Calabrian Margins (Central Mediterranean)" in Zenodo repository[29] (https://doi.org/10.5281/zenodo.17422269) and in the GeoscienceIR (https://geosciences-ir.it/en/) research infrastructure. The dataset[29] includes a geopackage file (named SLD – Submarine Landslide Database.gpkg) containing the three morphometrically characterized vector layers related to the scar crown, source area and deposit area of investigated submarine landslides (see Landslide mapping in Method section). Each single vector layer is even provided in shapefile format (.shp) and stored in a zip folder (SLD - Vector layer shapefiles) to make download easier. Furthermore, bathymetric data of the mapped submarine landslide source and deposit areas are provided at the highest available resolutions (5, 10, and 20 m) in a zip folder (SLD - Mapped landslide DEMs). All files are available in interoperable formats and projected in the international reference system WGS84 (EPSG: 4326).

## Technical Validation

Sources of uncertainty in the dataset are inherent to the following aspects.

**Bathymetric data uncertainty.** The completeness of a submarine landslide database is strongly affected by the uncertainty associated with bathymetric data, which is determined by its spatial resolution, accuracy and precision. These parameters can vary depending on factors such as water depth, instrumental specifications (e.g., beam density, signal frequency, acquisition geometry), and data processing methods[49].

Accuracy refers to how closely a measured or estimated value approximates the true bathymetric depth. In marine environments, accuracy is influenced by both the technical characteristics of the acquisition system and operational conditions during data collection. These factors collectively determine the potential deviation of the measured bathymetric surface from the actual seafloor morphology[49].

Precision reflects the repeatability of measurements obtained under identical conditions. For bathymetric data, precision is typically evaluated through repeated surveys of the same area. In the present study, however, precision could not be explicitly quantified because the dataset results from single-pass acquisitions, with no multi-temporal series available for independent comparison[49].

The spatial resolution of a bathymetric dataset is expressed as the distance between neighboring points in the grid in the X and Y axes[50]. Higher-resolution data can capture seafloor details, enabling the identification of small-scale geomorphological elements and a more accurate depiction of complex structures such as submarine landslides. Conversely, lower-resolution datasets may fail to resolve smaller features, leading to smoothing or coalescing of instability events, underestimating the true size, number and complexity of landslides.

To minimize potential biases, the bathymetric data employed in this study were acquired with careful consideration of all aspects related to survey planning. Specifically, calibration lines and subsequent acquisition lines were accurately designed, and sound velocity profiles (SVP) were collected to ensure compatibility with the spatial extent of the survey area. Swath overlaps were maintained within a range of 10–25%, thereby guaranteeing more than 100% coverage. Meteorological and sea-state conditions, as well as vessel motion, were continuously monitored and subsequently corrected by applying angular adjustments to pitch, roll, yaw, and heave parameters. Finally, for surveys conducted in water depths shallower than 200 m, tidal variations were accounted for by applying corrections based on tide gauge records from the Italian national monitoring network.

Overall, although precision cannot be formally evaluated due to the lack of repeated temporal measurements and minor accuracy-related uncertainties remain in the absence of direct ground-truth data, the standardized

| Operative parameters | | |
|---|---|---|
| **Parameters** | **Unit of measurement** | **Description** |
| * ID | // | Sequential number of each submarine landslide feature entry in the database. |
| * MatchingID | // | Unique number that identify the different portion of the same landslide (relation key). |
| * Physiographic domain | // | Physiographical domain of the seafloor where the submarine landslide has occurred. |
| * Repository | // | Metadata source of the data from past research that engaged the mapped features. |
| * Reference_1 | // | Peer-reviewed pubblication title, link or DOI that worked on the specific mapped features, n.1. |
| * Reference_2 | // | Peer-reviewed pubblication title, link or DOI that worked on the specific mapped features, n.2. |
| **Scar/Crown** | | |
| **Parameters** | **Unit of measurement** | **Description** |
| Max_Depth | m | Maximum water depth for the mapped submarine landslide scar crown limit. |
| Min_Depth | m | Minimum water depth for the mapped submarine landslide scar crown limit. |
| Scar_Length | m | Length of the mapped scar crown limit |
| Scar_Length3D | m | Length of the mapped scar crown limit, measured using the topographic surface. |
| * Max_Height | m | Height difference between the headscarp maximum convex point and the maximum concave point. |
| * Avg_Height | m | Mean height of the submarine landslide headscarp. |
| Bearing | deg | Horizontal direction of scar crown in realtion to the geographical north. |
| Sinuosity | Adimensional | Ratio of the curvilinear length and the Euclidean distance between the end points of the curve. |
| Max_Slope | deg | Maximum slope value of the submarine landslide headscarp. |
| * Ext_Slope | deg | Average value of the slope measured on a non-displaced portion of seafloor, close to the event. |
| * DEM_resolution | m | Horizontal resolution of the Digital Elevation Model in corrispondence of the mapped feature. |
| **Source area** | | |
| **Parameters** | **Unit of measurement** | **Description** |
| Max_Depth | m | Maximum water depth for the mapped submarine landslide scar crown limit. |
| Min_Depth | m | Minimum water depth for the mapped submarine landslide scar crown limit. |
| Perimeter | km | Measured perimeter of the submarine landslide deposit polygon. |
| Area | $km^2$ | Measured area of the submarine landslide deposit. |
| Area3D | $km^2$ | Measured topographic surface of the submarine landslide deposit area. |
| Volume | $km^3$ | Calculated volume of the Source area. |
| Aspect | deg | Direction of the topographic slope respect to the north. |
| * Length | m | Maximum length of the deposit area, measured following the flow direction. |
| * Width | m | Maximum width of the deposit area, measured perpendicularly to the length. |
| Max_Slope | deg | Maximum slope of the deposit area. |
| * Avg_Slope | deg | Average slope of the source area. |
| * DEM_resolution | m | Horizontal resolution of the Digital Elevation Model in corrispondence of the mapped feature. |
| **Deposit area** | | |
| **Parameters** | **Unit of measurement** | **Description** |
| Max_Depth | m | Maximum water depth for the mapped submarine landslide deposit area. |
| Min_Depth | m | Minimum water depth for the mapped submarine landslide deposit area. |
| Perimeter | km | Measured perimeter of the submarine landslide deposit polygon. |
| Area | $km^2$ | Measured area of the submarine landslide deposit. |
| Area3D | $km^2$ | Measured topographic surface of the submarine landslide deposit area. |
| Aspect | m | Direction of the topographic slope respect to the north. |
| * Length | m | Maximum length of the deposit area, measured following the ow direction. |
| * Width | m | Maximum width of the deposit area, measured perpendicularly to the length. |
| Max_Slope | deg | Maximum slope of the deposit area. |
| * Slope_Toe | deg | Measured slope in front of the toe outside the deposit area. |
| * DEM_resolution | m | Horizontal resolution of the Digital Elevation Model in corrispondence of the mapped feature. |

**Table 1.** List of the attributes included in the database[29]. Each vector layer consists of operative parameters and the related layer morphometric parameters highlighted with different colors. The manually inserted attributes are indicated by an *, while the others are automatically calculated during mapping or with field calculator.

acquisition procedures, together with the high spatial resolution of the bathymetric dataset, ensure a robust and reliable foundation for geomorphological characterization and subsequent analyses.

**Mapping procedure.** As already pointed out in the introduction, the non-automatic interpretation of DEM to identify submarine landslides features is inherently affected by significant variability, particularly when mapping is conducted by multiple operators with not standardized visualization settings. Moreover, it is highly dependent on the resolution of the DEM and the observation scale (i.e. scale of the interpreter's screen). To ensure consistent and accurate interpretation of submarine landslide features and to minimize both the overrepresentation and omission of

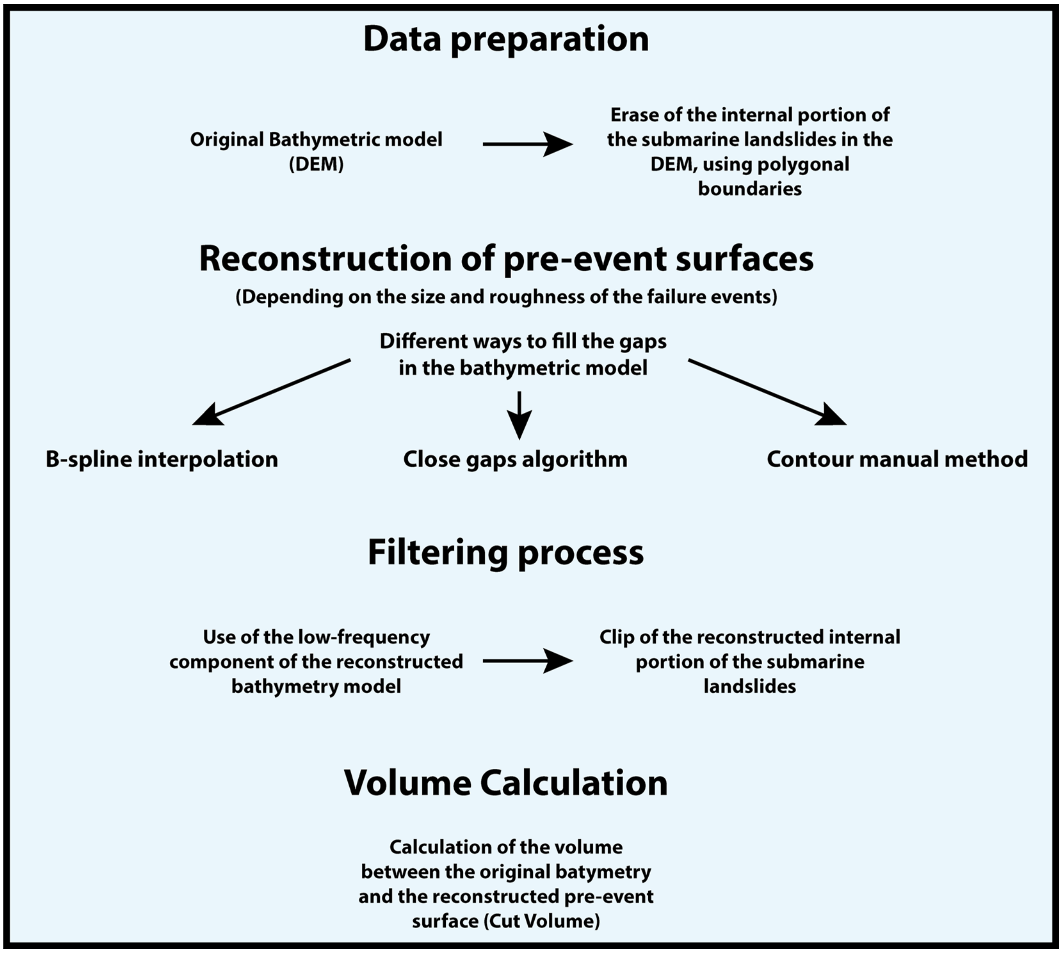


**Fig. 3** Workflow of the submarine landslide volume calculation.

morphological details, a standardized set of display parameters was defined and applied uniformly across the different digital elevation model (DEM) resolution classes. Specifically, for each grid resolution (5 m, 10 m, and 20 m), a fixed observation scale was adopted: 1:5,000 for the 5 m DEM, 1:10,000 for the 10 m DEM, and 1:20,000 for the 20 m DEM. These scales were selected to optimize the balance between spatial resolution and visual interpretability on screen, thereby enabling a consistent comparative analysis of features across the dataset. To further enhance the visibility of subtle topographic variations, a vertical exaggeration factor of 25 × was applied across all resolution classes. This level of exaggeration proved to be effective in emphasizing low-relief morphologies associated with submarine landslide features. Hillshade rendering was standardized using a zenithal illumination setup, which eliminates directional shading and provides a neutral lighting environment. While this configuration does not produce lateral shadows, when combined with high vertical exaggeration it allows for a clear and unbiased representation of slope breaks and scar edges. This approach ensured uniformity in feature detection and facilitated the comparison of geomorphic elements across the different DEM resolutions. Among the three mapped components of each landslide (scar/crown, evacuation area, and deposit), the scar or crown is generally the least problematic to delineate. However, some ambiguity may arise due to (1) the presence of multiple slope breaks, particularly when the uppermost break is smoothed or coalesced with others, and (2) the difficulty in identifying lateral terminations. In contrast, the deposit area proved to be the most challenging to delineate. Only 18 deposits (<1% of the total mapped landslides) were clearly identifiable and thus included in the database. Given that in most submarine landslides the failed mass evolves into a gravity flow and is therefore not preserved at the foot of the scar, when the deposit (or part of it) is observable, the main difficulties encountered are: (1) partial overlap of the deposit with the evacuation area, (2) complete or partial burial of the deposit, and (3) highly irregular or eroded terrain, which obscures the boundaries between landslide deposits and the surrounding seafloor.

**Volume estimation uncertainty.** Volume estimation for the submarine landslide database posed a significant challenge due to the high morphological variability of the submarine landslide features. As detailed in the Method section, volume estimation was realized by reconstructing the pre-failure surface of each scar using automated interpolation tools and subsequently computing the difference between the reconstructed and the real seafloor surfaces. This process inherently introduces an internal uncertainty, due to the assumption that the reconstructed surface represents the pre-failure topography. Moreover, the volume may be underestimated if the landslide deposit was not fully evacuated. Assessing the uncertainty associated with volume estimation is therefore crucial to quantify the robustness of the reconstruction methodologies.

To this end, the calculated volumes, using two distinct automatic morphological reconstruction approaches, were compared: the multilevel B-spline method and the Close Gap method. For each landslide in the database, the absolute and relative uncertainty was calculated based on the difference between the two volumes (Tab. 1S). Despite the methodological differences between the two approaches, frequency histograms of the estimated volumes show nearly identical distributions, both in shape and in key statistical descriptors (e.g., mean and median) (Fig. 3S), highlighting the overall consistency of the two techniques. The cumulative frequency analysis of relative uncertainty further reveals that approximately 80% of cases show a level of uncertainty lower than 30%, indicating a high degree of agreement between the two reconstruction methods (Fig. 4S). These findings support the reliability of the volume estimation approach and indicate that methodological differences have a minimal impact on the final volume calculations.

**Content harmonization.** In addition to the standardization and error reduction processes already carried out by the authors, the content of the database[29] of submarine landslides underwent to a data harmonization process carried out to fit in the research infrastructure "GeoscienceIR." The attribute fields of each layer were structured to ensure the best possible understanding of the attribute contents (avoiding abbreviations). Furthermore, a codelist was created for the categorized attribute (in our case the "Physiographic domain"), and relationship keys were defined between the layers of the database[29]. This step ensures consistency, interoperability, and seamless integration with other datasets and systems within the research infrastructure.

**Representativeness of the data records.** The submarine landslide database[29] developed in this study represents a step toward the understanding of the spatial distribution of gravitational instabilities along the Calabrian continental margins. The structure and content of the database not only develop a national inventory of submarine landslides but is also particularly suitable for a range of applied studies. Notably, the inclusion of calculated landslide volumes, as well as detailed depth and slope metrics, makes the dataset valuable for numerical modeling of landslide-induced tsunamis, as highlighted in previous studies[17,51,52]. Another promising application of the database is the assessment of landslide susceptibility, representing the probability of landslide occurrence in a given area under specific conditions. Susceptibility analyses in the submarine environment are still relatively rare and underdeveloped, primarily due to the intrinsic challenges of data acquisition in deep marine settings and the difficulty in collecting large and representative samples of events. As a result, only a limited number of studies addressing submarine landslide susceptibility were found in the literature[53–56].

## Usage Notes

The Submarine landslide database[29] is a FAIR product developed within the framework of the "GeoscienceIR" project, available to all researchers and professionals in marine sciences, particularly those interested in submarine landslides. The data provided was produced using the software Global Mapper v.25. However, the mapping work and measurement of attributes can easily be performed by using open-source software such as QGIS. The volume calculations were developed using SAGA tools (https://saga-gis.sourceforge.io/en/index.html) in QGIS. The content of the Submarine landslide database[29] is structured to ensure interoperability and reproducibility across different GIS software platforms. The database[29] we realized show intrinsic limitations because it is based on bathymetric data that are not able to give all the information about the instability events. Therefore, the database will be continuously updated through the help of marine scientific community, with the aim to expand the investigated area to achieve national-scale mapping and incorporate further data from different sources.

## Data availability

The dataset used in this study is publicly available in the Zenodo repository (https://doi.org/10.5281/zenodo.17422269) under the title "Submarine Landslides Database along the Calabrian Margins (Central Mediterranean)" and through the GeoscienceIR research infrastructure (https://geosciences-ir.it/en/).

## Code availability

No customized code was used to produce the dataset.

Received: 24 June 2025; Accepted: 3 November 2025;
Published online: 17 December 2025

## References

1. Hühnerbach, V. & Masson, D. G. Landslides in the North Atlantic and its adjacent seas: an analysis of their morphology, setting and behaviour. *Marine Geology* **213**, 343–362, https://doi.org/10.1016/j.margeo.2004.10.013 (2004).
2. Micallef, A., Mountjoy, J. J., Canals, M. & Lastras, G. in *Submarine Mass Movements and Their Consequences* Ch. Chapter 18, 201-212 (2012).
3. Mueller, R. Response to comments by on "Evidence for the biotic origin of seabed pockmarks on the Australian continental shelf. *Marine and Petroleum Geology* **69**, 262–265 (2016).
4. Lastras, G., Amblas, D., Canals, M. & Party, D. S. Fjord-flank collapse and associated deformation in Aysén Fjord, Chile (2016).
5. Terrinha, P. *et al.* The Tagus River delta landslide, off Lisbon, Portugal. Implications for marine geo-hazards. *Marine Geology* **416**, 105983 (2019).
6. L'Heureux, J.-S., Hansen, L., Longva, O., Emdal, A. & Grande, L. O. A multidisciplinary study of submarine landslides at the Nidelva fjord delta, Central Norway-Implications for geohazard assessment. *Norwegian Journal of Geology* **90**, 1–20 (2010).
7. McAdoo, B. G., Pratson, L. F. & Orange, D. L. Submarine landslide geomorphology, US continental slope. *Marine geology* **169**, 103–136 (2000).
8. Krastel, S. *et al.* Submarine landslides around the Canary Islands. *Journal of Geophysical Research: Solid Earth* **106**, 3977–3997 (2001).

9. Watt, S. F. L., Talling, P. J. & Hunt, J. E. New insights into the emplacement dynamics of volcanic island landslides. *Oceanography* **27**, 46–57 (2014).
10. Ercilla, G. & Casas, D. Submarine mass movements: sedimentary characterization and controlling factors. *Earth Sciences* **3**, 99–128 (2012).
11. Nawanao, L. P. Jr & Ramos, N. T. Frontal wedge variations and controls of submarine landslides in the Negros–Sulu Trench System, Philippines. *Frontiers in Earth Science* **11**, 1054825 (2023).
12. Prior, D. B. & Coleman, J. M. Submarine landslides-geometry and nomenclature. *Zeitschrift für Geomorphologie Stuttgart* **23**, 415–426 (1979).
13. Yang, Y., Yang, J., Li, W. & Jing, S. Slope instability and submarine-moat initiation: Insights from the northern South China sea margin. *Marine and Petroleum Geology* **160**, 106610 (2024).
14. Sun, M., Liu, Y., Zhao, L., Xie, W. & Mao, W. Advances and challenges in assessing submarine landslide risks to marine infrastructure. *Natural Hazards*, 1-27 (2025).
15. Colantoni, P. *et al. Processi Dinamici Del Canyon Sottomarino de Gioia Tauro (Mare Tirreno)* (1992).
16. Huang, Y. & Jin, P. Impact of human interventions on coastal and marine geological hazards: a review. *Bulletin of Engineering Geology and the Environment* **77**, 1081–1090 (2018).
17. Zaniboni, F., Armigliato, A., Pagnoni, G. & Tinti, S. Continental margins as a source of tsunami hazard: the 1977 Gioia Tauro (Italy) landslide–tsunami investigated through numerical modeling. *Marine Geology* **357**, 210–217 (2014).
18. Assier-Rzadkieaicz, S., Heinrich, P., Sabatier, P. C., Savoye, B. & Bourillet, J. F. Numerical modelling of a landslide-generated tsunami: the 1979 Nice event. *Pure and Applied Geophysics* **157**, 1707–1727 (2000).
19. Du, P. *et al.* Earthquake-induced Submarine Landslides (EQISLs) and a comparison with their Terrestrial Counterparts: Insights from a New Database. *Earth-Science Reviews* **261**, 105021 (2025).
20. Twichell, D. C., Chaytor, J. D., ten Brink, U. S. & Buczkowski, B. Morphology of late Quaternary submarine landslides along the U.S. Atlantic continental margin. *Marine Geology* **264**, 4–15, https://doi.org/10.1016/j.margeo.2009.01.009 (2009).
21. Chaytor, J. D., ten Brink, U. S., Solow, A. R. & Andrews, B. D. Size distribution of submarine landslides along the U.S. Atlantic margin. *Marine Geology* **264**, 16–27, https://doi.org/10.1016/j.margeo.2008.08.007 (2009).
22. Urgeles, R. & Camerlenghi, A. Submarine landslides of the Mediterranean Sea: Trigger mechanisms, dynamics, and frequency-magnitude distribution. *Journal of Geophysical Research: Earth Surface* **118**, 2600–2618, https://doi.org/10.1002/2013JF002720 (2013).
23. Borrell, N. *et al.* in *Submarine Mass Movements and their Consequences Advances in Natural and Technological Hazards Research* Ch. Chapter 50, 499-508 (2016).
24. León, R. *et al.* Geological and tectonic controls on morphometrics of submarine landslides of the Spanish margins. *Geological Society, London, Special Publications* **500**, 495–513, https://doi.org/10.1144/sp500-2019-153 (2020).
25. Gamboa, D., Omira, R. & Terrinha, P. A database of submarine landslides offshore West and Southwest Iberia. *Sci Data* **8**, 185, https://doi.org/10.1038/s41597-021-00969-w (2021).
26. Clarke, S. L., Hubble, T. C. T., Miao, G., Airey, D. W. & Ward, S. N. Eastern Australia's submarine landslides: implications for tsunami hazard between Jervis Bay and Fraser Island. *Landslides* **16**, 2059–2085, https://doi.org/10.1007/s10346-019-01223-6 (2019).
27. Puga-Bernabéu, Á., López-Cabrera, J., Webster, J. M. & Beaman, R. J. Submarine landslide morphometrics and slope failure dynamics along a mixed carbonate-siliciclastic margin, north-eastern Australia. *Geomorphology* **403**, https://doi.org/10.1016/j.geomorph.2022.108179 (2022).
28. Chiocci, F. L. & Ridente, D. Regional-scale seafloor mapping and geohazard assessment. The experience from the Italian project MaGIC (Marine Geohazards along the Italian Coasts). *Marine Geophysical Research* **32**, 13–23 (2011).
29. Bianchini, M., Ceramicola, S., & Chiocci, F. L. Submarine Landslides Database along the Calabrian Margins (Central Mediterranean) *Zenodo*, https://doi.org/10.5281/zenodo.17422269 (2025).
30. Casalbore, D. *et al.* Geohazard features of the Tyrrhenian Calabria. *Journal of Maps* **20**, https://doi.org/10.1080/17445647.2024.2347897 (2024).
31. Ceramicola, S. *et al.* Geohazard features of the Ionian Calabrian margin. *Journal of Maps* **20**, 2349785 (2024).
32. Corradino, M. *et al.* Active tectonics in the Calabrian Arc: Insights from the Late Miocene to Recent structural evolution of the Squillace Basin (offshore eastern Calabria). *Tectonophysics* **851**, 229772 (2023).
33. Malinverno, A. & Ryan, W. B. F. Extension in the Tyrrhenian Sea and shortening in the Apennines as result of arc migration driven by sinking of the lithosphere. *Tectonics* **5**, 227–245 (1986).
34. Sgroi, T., Polonia, A., Barberi, G., Billi, A. & Gasperini, L. New seismological data from the Calabrian arc reveal arc-orthogonal extension across the subduction zone. *Scientific Reports* **11**, 473 (2021).
35. Antonioli, F. *et al.* Late Pleistocene to Holocene record of changing uplift rates in southern Calabria and northeastern Sicily (southern Italy, Central Mediterranean Sea). *Tectonophysics* **422**, 23–40 (2006).
36. Zecchin, M. *et al.* The Plio-Pleistocene evolution of the Crotone Basin (southern Italy): interplay between sedimentation, tectonics and eustasy in the frame of Calabrian Arc migration. *Earth-Science Reviews* **115**, 273–303 (2012).
37. Ferranti, L., Antonioli, F., Anzidei, M., Monaco, C. & Stocchi, P. The timescale and spatial extent of vertical tectonic motions in Italy: insights from relative sea-level changes studies. *Journal of the Virtual Explorer* **36** (2010).
38. Prada, M. *et al.* The structure of Mediterranean arcs: New insights from the Calabrian Arc subduction system. *Earth and Planetary Science Letters* **548**, 116480 (2020).
39. Loreto, M. F., Zitellini, N., Ranero, C. R., Palmiotto, C. & Prada, M. Extensional tectonics during the Tyrrhenian back-arc basin formation and a new morpho-tectonic map. *Basin Research* **33**, 138–158, https://doi.org/10.1111/bre.12458 (2020).
40. Casalbore, D., Bosman, A., Ridente, D. & Chiocci, F. L. in *Submarine Mass Movements and Their Consequences: 6th International Symposium* (eds Sebastian Krastel *et al.*) 261–269 (Springer International Publishing, 2014).
41. Ceramicola, S. *et al.* in *Landslide Science for a Safer Geoenvironment* Ch. Chapter 85, 557-562 (2014).
42. Huhn, K. *et al.* Modern submarine landslide complexes: a short review. *Submarine landslides: Subaqueous mass transport deposits from outcrops to seismic profiles*, 181–200 (2019).
43. Westaway, R. Quaternary uplift of southern Italy. *Journal of Geophysical Research: Solid Earth* **98**, 21741–21772 (1993).
44. Ferranti, L., Monaco, C., Morelli, D., Antonioli, F. & Maschio, L. Holocene activity of the Scilla Fault, Southern Calabria: Insights from coastal morphological and structural investigations. *Tectonophysics* **453**, 74–93 (2008).
45. Chiocci, F. L., Budillon, F., Ceramicola, S. & Orrù, F. G. *Atlante dei lineamenti di pericolosità geologica dei mari italiani-Risultati del progetto MaGIC*. (CNR edizioni, 2021).
46. Clare, M. *et al.* A consistent global approach for the morphometric characterization of subaqueous landslides. *Geological Society, London, Special Publications* **477**, 455–477 (2019).
47. Lee, S., Wolberg, G. & Shin, S. Y. Scattered data interpolation with multilevel B-splines. *IEEE transactions on visualization and computer graphics* **3**, 228–244 (1997).
48. Conrad, O. SAGA–program structure and current state of implementation. *Göttinger Geographische Abhandlungen* **115**, 39–52 (2006).
49. Li, Z. *et al.* Exploring modern bathymetry: A comprehensive review of data acquisition devices, model accuracy, and interpolation techniques for enhanced underwater mapping. *Frontiers in Marine Science* **10**, 1178845 (2023).
50. Maleika, W. The influence of the grid resolution on the accuracy of the digital terrain model used in seabed modeling. *Marine Geophysical Research* **36**, 35–44 (2015).
51. Zaniboni, F. *et al.* Assessment of the 1783 Scilla landslide–tsunami's effects on the Calabrian and Sicilian coasts through numerical modeling. *Natural Hazards and Earth System Sciences* **19**, 1585–1600 (2019).

52. McAdoo, B. G. & Watts, P. Tsunami hazard from submarine landslides on the Oregon continental slope. *Marine Geology* **203**, 235–245, https://doi.org/10.1016/S0025-3227(03)00307-4 (2004).
53. Innocenti, C., Battaglini, L., D'Angelo, S. & Fiorentino, A. Submarine landslides: mapping the susceptibility in European seas. *Quarterly Journal of Engineering Geology and Hydrogeology* **54**, https://doi.org/10.1144/qjegh2020-027 (2020).
54. Nian, T.-k., Guo, X.-s., Zheng, D.-f., Xiu, Z.-x. & Jiang, Z.-b. Susceptibility assessment of regional submarine landslides triggered by seismic actions. *Applied Ocean Research* **93**, https://doi.org/10.1016/j.apor.2019.101964 (2019).
55. Avdievitch, N. N. & Coe, J. A. Submarine Landslide Susceptibility Mapping in Recently Deglaciated Terrain, Glacier Bay, Alaska. *Frontiers in Earth Science* **10**, https://doi.org/10.3389/feart.2022.821188 (2022).
56. Scacchia, E. *et al*. Shallow-Water Submarine Landslide Susceptibility Map: The Example in a Sector of Capo d'Orlando Continental Margin (Southern Tyrrhenian Sea). *Journal of Marine Science and Engineering* **13**, 1350 (2025).


## Acknowledgements

The present work is supported by the project "GeoscienceIR, funded by European Union - NextGenerationEU - Mission 4 "Education and Research" - Component 2 "From Research to Business" - Investment 3.1 "Fund for the realization of an integrated system of research and innovation infrastructures" - Project IR0000037 - GeoSciences IR - CUP I53C22000800006. We are grateful to the two anonymous reviewers and editors for their careful revisions that largely improved the quality of the paper.

## Author contributions

Marco Bianchini: Writing – review & editing, Writing – original draft, Supervision, Methodology, Investigation, Data curation, Conceptualization. Francesco Latino Chiocci: Review & editing. Silvia Ceramicola: Review & editing, Supervision.

## Competing interests

The authors declare that the research was conducted in the absence of any commercial or financial relationships that could be construed as a potential conflict of interest.

## Additional information

**Supplementary information** The online version contains supplementary material available at https://doi.org/10.1038/s41597-025-06239-3.

**Correspondence** and requests for materials should be addressed to M.B.